JOURNAL OF ENZYME INHIBITION AND MEDICINAL CHEMISTRY
2023, VOL. 388, NO. 1, 2231170
https://doi.org/10.1080/14756366.2023.2231170

Taylor & Francis
Taylor & Francis Group

RESEARCH ARTICLE

OPEN ACCESS Check for updates

Development of new thiazolidine-2,4-dione hybrids as aldose reductase inhibitors endowed with antihyperglycaemic activity: design, synthesis, biological investigations, and *in silico* insights

Abdelrahman Hamdi[a], Muhammad Yaseen[b], Wafaa A. Ewes[a], Mashooq Ahmad Bhat[c], Noha I. Ziedan[d], Hamed W. El-Shafey[a], Ahmed A. B. Mohamed[e], Mohamed R. Elnagar[f,g], Abdullah Haikal[h], Dina I. A. Othman[a], Abdullah A. Elgazar[i], Ahmed H. A. Abusabaa[j], Kamal S. Abdelrahman[k], Osama M. Soltan[k] and Mostafa M. Elbadawi[l]

[a]Department of Pharmaceutical Organic Chemistry, Faculty of Pharmacy, Mansoura University, Mansoura, Egypt; [b]Institute of Chemical Sciences, University of Swat, Swat, Pakistan; [c]Department of Pharmaceutical Chemistry, College of Pharmacy, King Saud University, Riyadh, Saudi Arabia; [d]Department of physical, mathematical and Engineering science, Faculty of science, Business and Enterprise, University of Chester, Chester, UK; [e]Department of Medicinal Chemistry, Faculty of Pharmacy, Mansoura University, Mansoura, Egypt; [f]Pharmacology and Toxicology Department, Faculty of Pharmacy, Al-Azhar University, Cairo, Egypt; [g]Department of Pharmacology, College of Pharmacy, The Islamic University, Najaf, Iraq; [h]Department of Pharmacognosy, Faculty of Pharmacy, Mansoura University, Mansoura, Egypt; [i]Department of Pharmacognosy, Faculty of Pharmacy, Kafrelsheikh University, Kafrelsheikh, Egypt; [j]Department of Organic and Medicinal Chemistry, Faculty of Pharmacy, Fayoum University, Fayoum, Egypt; [k]Department of Pharmaceutical Chemistry, Faculty of Pharmacy, Al-Azhar University, Assiut, Egypt; [l]Department of Pharmaceutical Chemistry, Faculty of Pharmacy, Kafrelsheikh University, Kafrelsheikh, Egypt

ABSTRACT

This research study describes the development of new small molecules based on 2,4-thiazolidinedione (2,4-TZD) and their aldose reductase (AR) inhibitory activities. The synthesis of 17 new derivatives of 2,4-TZDs hybrids was feasible by incorporating two known bioactive scaffolds, benzothiazole heterocycle, and nitro phenacyl moiety. The most active hybrid (**8b**) was found to inhibit AR in a non-competitive manner (0.16 µM), as confirmed by kinetic studies and molecular docking simulations. Furthermore, the *in vivo* experiments demonstrated that compound **8b** had a significant hypoglycaemic effect in mice with hyperglycaemia induced by streptozotocin. Fifty milligrams per kilogram dose of **8b** produced a marked decrease in blood glucose concentration, and a lower dose of 5 mg/kg demonstrated a noticeable antihyperglycaemic effect. These outcomes suggested that compound **8b** may be used as a promising therapeutic agent for the treatment of diabetic complications.

ARTICLE HISTORY
Received 24 May 2023
Revised 23 June 2023
Accepted 25 June 2023

KEYWORDS
Thiazolidinone-2,4-diones; benzothiazole; aldose reductase inhibition; antihyperglycaemic; docking

Introduction

Diabetes mellitus is a major cause of several progressive and chronic diseases that adversely affect many organs, including vascular and nervous systems, with an approximated 200 million causalities of mortality and morbidity[1,2]. Type 2 diabetes (T2D) is a chronic life-threatening disorder exhibiting abnormal elevated blood glucose (BG) concentration resulting from diminished response of the target tissues to insulin action (insulin resistance) and progressive impaired function of β cells in pancreas[2,3]. Thus, diabetes is considered a major and growing public health burden, and has gained prime global health importance because of the several long-term complications, such as neuropathy, nephropathy, retinopathy, cataract, and cardiovascular disorders[3,4]. Most of the currently available drugs can cause problems including hypoglycaemia, compliance, and obesity[5,6]. Hence, there is a crucial necessity to develop new safe and potent antidiabetic drugs with improved compliance and reduced side effects[3,4].

Under hyperglycaemic state, higher than 30% of the BG is bio--transformed into sorbitol by aldose reductase (AR) enzyme resulting in the major diabetic secondary complications[7–11]. Subsequently, sorbitol dehydrogenase converts sorbitol to fructose through polyol pathway, which is a necessary mechanism for regulation of glucose metabolism in mammalian cells. AR is a key enzyme that belongs to aldo-keto reductase super-family involved in the polyol pathway for glucose reduction to sorbitol (Figure 1). It is believed that activation of this metabolic pathway is associated with the chronic diabetic complications like retinopathy, diabetic cataract, neuropathy, and nephropathy. Therefore, aldose reductase inhibitors (ARIs) emerged as a fruitful therapeutic tool to prevent the development of these metabolic complications via inhibition of the first step of polyol pathway[1,7,8]. ARIs have been found to supress and prevent sorbitol accumulation in specific tissues such as peripheral nerves, lens, and kidney. Accordingly, the decreased sorbitol flux by ARIs could be exploited as emerging

CONTACT Abdelrahman Hamdi abdelrahmanhamdi2012@yahoo.com Department of Pharmaceutical Organic Chemistry, Faculty of Pharmacy, Mansoura University, Mansoura, Egypt; Muhammad Yaseen muhammadyaseen.my907@gmail.com Institute of Chemical Sciences, University of Swat, Main Campus, Charbagh, Swat, Pakistan

Supplemental data for this article can be accessed online at https://doi.org/10.1080/14756366.2023.2231170.

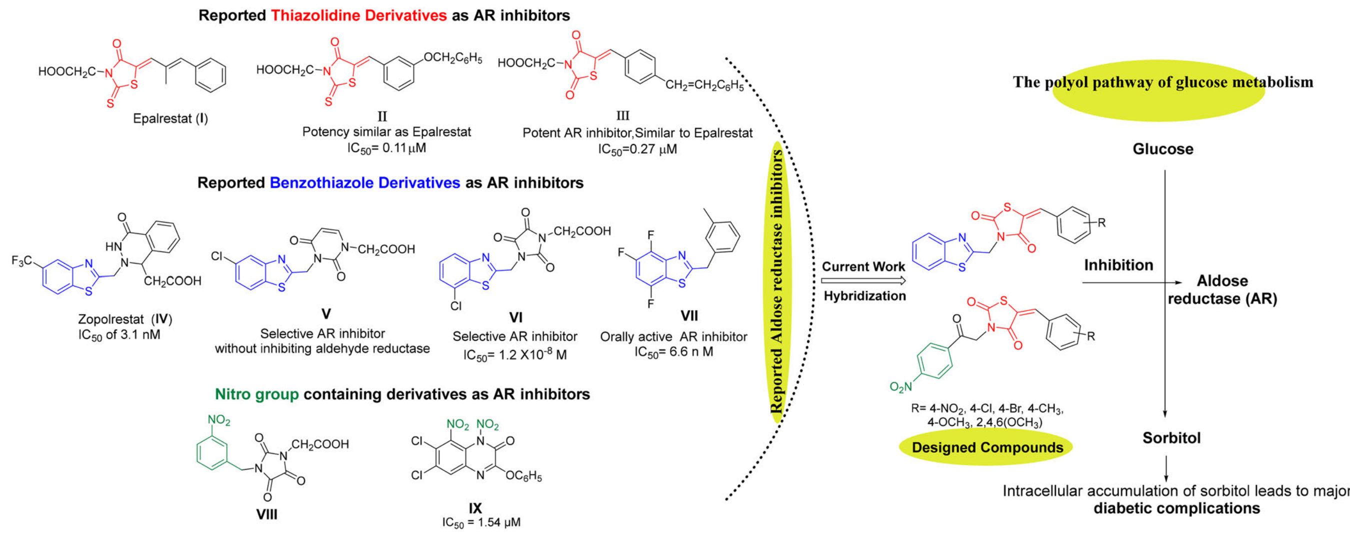

Figure 1. Design of new 5-arylidene-2,4-TZDs-based hybrids as ARIs based on some reported AR inhibitors.

approach for the management of major diabetes complications. Furthermore, the pathogenesis of sorbitol-induced diabetic complications may be result from interruption in cellular redox, sorbitol-osmotic effects, free radical defence, in addition to elevated oxidative and glycation stress[1].

Orally active ARIs vary structurally and are classified into two major chemical groups: cyclic imides (mainly spirohydantoins) and carboxylic acid derivatives, such as Epalrestat (**I**)[4]. The majority of carboxylic acid derivatives were evaluated as ARIs preclinically and clinically, nonetheless, their development is generally restrained by their diminished *in vivo* potency, several side effects, and pharmacokinetic obstacles[12,13]. The carboxylic acid ARIs show potent *in vitro* activity as ARIs; however, their effectiveness decreases *in vivo*. Carboxylic acid derivatives could be completely ionised at physiological pH, and thus, their *in vivo* activity is generally lower than that of less ionised compounds. This effect is possibly due to the impaired penetration of physiological membranes of such ionised compounds[14–16]. Therefore, the development of a new generation of more selective non-carboxylic acid ARIs is prioritised to pursue the desired pharmacokinetic and therapeutic properties with reduced toxicity, fewer side effects and enhanced tissue permeability and drug uptake at the physiological pH. Currently, Epalrestat (**I**), which is a carboxylic acid derivative bearing 2-thioxo-4-thiazolidinone moiety (Figure 1), is the only approved ARI commercially available in Japan, China, and India. Epalrestat (**I**) is easily absorbed into the neural tissue and inhibits AR with minimum side effects[17–19].

Likewise, there is a great interest in 2,4-thiazolidinediones (2,4-TZDs) as a new class of antidiabetic drugs acting as ARIs with dual activity controlling both glucose and lipid metabolism[12]. 2,4-TZDs, as antidiabetic agent, has been previously reported to act by activating peroxisome proliferator-activated receptors (PPARs), specifically PPAR-gamma (PPARγ). Upon activation of these receptors, increasing transcription of a number of specific genes and decreasing transcription of others would happen. As a result, these receptors play transcriptional regulation of some genes and in turn control glucose and lipid metabolism. Briefly, the main effect of expression and repression of these receptors is an increase in the storage of fatty acids in adipocytes, and thereby decreasing the amount of fatty acids existing in the circulation. Thus, cells become more dependent on the oxidation of glucose to provide energy for other cellular processes[12].

As a result, 2,4-TZDs are efficient in metabolic regulation of lipid and glucose associated with insulin resistance and therefore, they markedly differ from other antihyperglycaemic agents in having dual activity used for the treatment of both T2D and obesity[12,20,21]. Interestingly, several 5-arylidene-2,4-TZDs such as compound **II** and **III** (Figure 1) have been reported as safer bioisosteres of the other AR inhibitors and have exerted appreciable AR inhibitory activities[22,23].

Furthermore, benzothiazole-based carboxylic acids, such as Zopolrestat (**IV**), have shown potent and selective inhibition of AR (Figure 1). Zopolrestat is a potent, orally active AR inhibitor used for the treatment of diabetic complications with IC_{50} value of 3.1 nM[24,25]. Thus, benzothiazole side chains featured in Zopolrestat were then incorporated into several other derivatives, such as compounds **V**, **VI**, and **VII**, which have been proved to show potent AR inhibition activities[12,26–30].

Moreover, several molecules containing nitro group, for example, aromatic nitro compounds **VIII** and **IX**, have discovered with potential AR inhibitory activity (Figure 1). The nitro group was anticipated to play an important role for AR active site binding interactions with Tyr48 and His110 residues, which are the residues essential for binding with carboxylic acids ARIs through their anionic forms[13,31,32].

In the present study and in the light of the aforesaid investigations, the structure features of our designed compounds were based on the reported AR inhibitory abilities of 5-arylidene-2,4-TZDs pharmacophore as well as benzothiazole nucleus and aromatic nitro compounds (Figure 1). For this endeavour, 5-arylidene-2,4-TZDs-based derivatives as a privileged scaffold, have been designed, synthesised, and biologically evaluated for their AR inhibitory impact. As well, based on a hybrid pharmacophore design, the incorporation of benzothiazole or nitro phenyl moieties was hoped to generate new hybrid candidates with better AR inhibition[4]. The present study focuses on the synthesis of 5-arylidene-2,4-TZDs hybrids substituted at position 3 with either benzothiazole pharmacophore or 4-nitrophenyl-2-oxoethyl substituent in an attempt to investigate the role of these versatile bioactive functionalities in AR inhibition (Figure 1). Finally, all the synthesised compounds were investigated for their potential to inhibit AR where the most active compound would be also evaluated for its antihyperglycaemic influence. Further, molecular docking studies were conducted to rationalise their possible binding interactions in AR binding site.

Results and discussion

Chemistry

The synthetic approach exploited for preparation of the target compounds, *(Z)-5-(4 or 3-substitutedbenzylidene)*-3-(2-(4-nitrophenyl)-2-oxoethyl)thiazolidine-2,4-dione (**5a**–**k**) and (Z)-3-(benzo[d]thiazol-2-ylmethyl)-5-(4-subtitutedbenzylidene)thiazolidine-2,4-dione (**8a**–**h**) is outlined in Schemes 1 and 2. The synthesis of *N*-unsubstituted 5-arylidene-thiazolidine-2,4-diones (**3a**–**k**) in acceptable yield has been accomplished employing Knoevenagel condensation, where the thiazolidine-2,4-dione was condensed with the corresponding arylaldehyde as reported previously[33–36]. After that, compounds **3a**–**k** were refluxed in ethanol with potassium hydroxide to obtain the subsequent potassium salts **4a**–**k**. After that, the potassium salts **4a**–**k** were stirred with 2-bromo-4′-nitroacetophenone in DMF to attain the corresponding derivatives **5a**–**k** (Scheme 1). On the other hand, the benzothiazole counterparts **8a**–**h** were synthesised through refluxing the potassium salts **4a**–**g** and **4l** with benzothiazole methyl chloride **7** in DMF (Scheme 2). The newly synthesised thiazolidine-2,4-dione hybrids **5a**–**k** and **8a**–**h** were elucidated utilising spectroscopic analyses (^{1}H NMR, ^{13}C NMR, and MS). All spectral and analytical results were compatible with the assigned compounds.

Regarding IR spectral data for the target, thiazolidine-2,4-dione hybrids **5a**–**k** and **8a**–**h** showed two strong absorption bands at 1754–1737 cm^{-1}, 1704–1687 cm^{-1} resulting from the starching of the two C=O in thiazolidine-2,4-dione scaffold. For ^{1}H NMR spectra of thiazolidine-2,4-diones **5a**–**k** and **8a**–**h**, they demonstrated one singlet signal around 8 ppm for the benzylidene proton that supported the occurrence of Knoevenagel reaction between 2,4-diones **3a**–**k** and the selected aromatic aldehydes. Also, the absence of a singlet signal corresponding to the NH from the thiazolidine-2,4-dione ring at 12.50–12.52 ppm confirmed the success of *N*-substitution of potassium salts **4a**–**k**.[37] Moreover, ^{1}H NMR spectral data of the hybrids **5a**–**k** and **8a**–**h** showed one signal for N-CH_2 methyl group as singlet signal around 5.4 ppm. Concerning ^{13}C NMR of the hybrids **5a**–**k** and **8a**–**h**, it was revealed that the appearance of either three or two signals at 170–157 ppm confirmed the presence of olefinic carbons. Moreover, the existence of one signal at about 45 ppm was assigned to the methyl carbon. Finally, the mass spectral data gave the fragmentation patterns of the target compounds and their corresponding mass revealing the molecular ion peaks (M^+) as predicted by their molecular formulas.

Biological evaluation

Inhibitory activity against human aldose reductase

All the newly synthesised thiazolidine-2,4-dione hybrids **5a**–**k** and **8a**–**h** were screened for their *in vitro* inhibitory activity against human AR using Epalrestat as a positive control. The results of *in vitro* AR inhibition activity are presented as IC_{50} values in Table 1. The obtained results indicated that the tested compounds demonstrated variable inhibitory potencies against AR enzyme at sub-micromolar level, except for compound **8a**. Regarding benzothiazole-tethered thiazolidine-2,4-dione **8b**, it was found to be the most potent AR inhibitor with IC_{50} of 0.16 μM, falling closer to Epalrestat reference drug (IC_{50} of 0.10 μM). Moreover, the

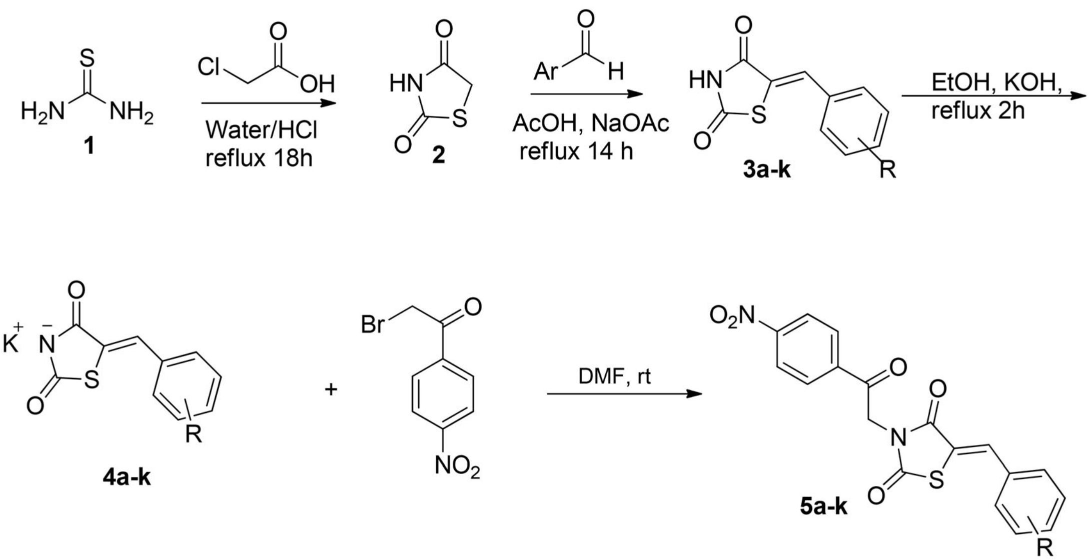

4a, R=4-NO_2
4b, R=4-Cl
4c, R=4-Br
4d, R=4-F
4e, R=4-CH_3
4f, R=4-OCH_3
4g, R=3,4,5(OCH_3)
4h, R=3-NO_2
4k, R=3-Br

5a, R=4-NO_2
5b, R=4-Cl
5c, R=4-Br
5d, R=4-F
5e, R=4-CH_3
5f, R=4-OCH_3
5g, R=3,4,5(OCH_3)
5h, R=3-NO_2
5k, R=3-Br

Scheme 1. Synthetic pathway for the target 4-nitro-phenacyl tethered thiazolidine-2,4-dione hybrids **5a**–**k**.

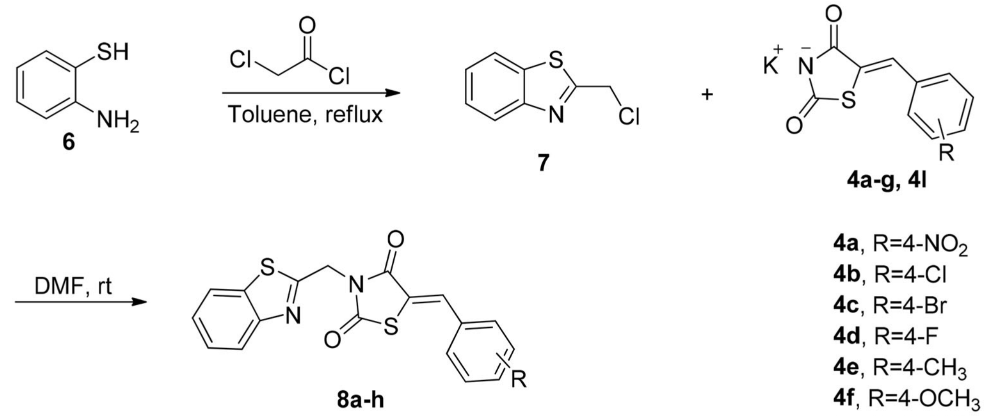

4a, R=4-NO_2
4b, R=4-Cl
4c, R=4-Br
4d, R=4-F
4e, R=4-CH_3
4f, R=4-OCH_3
4g, R=3,4,5(OCH_3)
4l, R=3,4(OCH_3)

8a, R=4-NO_2
8b, R=4-Cl
8c, R=4-Br
8d, R=4-F
8e, R=4-CH_3
8f, R=4-OCH_3
8g, R=3,4,5(OCH_3)
8h, R=3,4(OCH_3)

Scheme 2. Synthetic pathway for the target benzothiazole tethered thiazolidine-2,4-dione hybrids **8a**–**h**.

Table 1. IC_{50} values of the tested compounds **5a**–**k** and **8a**–**h** against human aldose reductase.

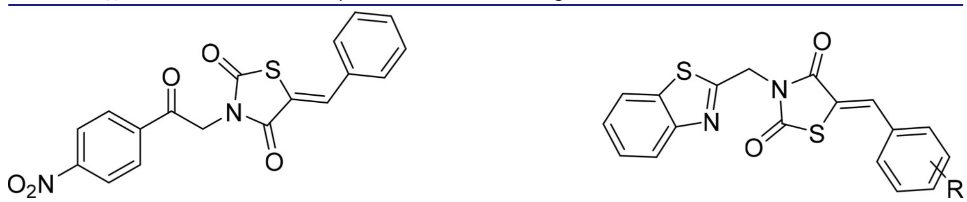

Comp.	R	AR inhibition, IC_{50} (μM)
5a	4-NO_2	0.22
5b	4-Cl	0.46
5c	4-Br	0.49
5d	4-F	0.57
5e	4-CH_3	0.55
5f	4-OCH_3	0.28
5g	3,4,5-triOCH_3	0.72
5h	3-NO_2	0.51
5k	3-Br	0.41
8a	4-NO_2	1.98
8b	4-Cl	0.16
8c	4-Br	0.21
8d	4-F	0.33
8e	4-CH_3	0.29
8f	4-OCH_3	0.94
8g	3,4,5-triOCH_3	0.27
8h	3,4-diOCH_3	0.45
Epalrestat	–	0.10

phenacyl-thiazolidine-2,4-dione hybrids **5a**, **5f** as well as the benzothiazole-based candidates **8c**, **8e**, and **8g** exhibited a strong inhibitory impact with IC_{50} range spanning from 0.21 μM to 0.29 μM. Furthermore, the phenacyl-derived hybrids **5b**–**e**, **5h**, and **5k** and the benzothiazole-based analogues **8d** and **8h** displayed moderate inhibitory effect with IC_{50} range from 0.33 to 0.57 μM. On contrary, the counterparts **5g**, **8a**, and **8f** showed weak inhibitory influence with IC_{50} range of 0.72–1.98 μM.

The SAR analysis for the assessed compounds hinted out that the enzyme inhibitory action is influenced by the various substituents appended to the aromatic ring of benzylidene moiety either in phenacyl-thiazolidine-2,4-dione hybrids **5a**–**k** or in benzothiazole-thiazolidine-2,4-dione hybrids **8a**–**h**. Regarding the phenacyl-derived thiazolidine-2,4-dione hybrids **5a**–**k**, the appending of NO_2 functionality to aromatic ring had a potential impact on AR inhibition (**5a**, IC_{50} = 0.22 μM) affording the highest potent AR inhibitor within these series. Of special note, shifting of NO_2 group to *meta* position to provide the regioisomer **5h** (IC_{50} = 0.51 μM) declined the inhibitory action by more than two-fold. In a similar behaviour, the inclusion of 4-chloro **5b**, 4-bromo **5c**, 4-fluoro **5d**, 4-methyl **5e**, or 3,4,5-OCH_3 **5g** to benzylidene moiety sharply reduced the AR inhibitory action (IC_{50} values equal 0.46, 0.49, 0.57, 0.55, and 0.72 μM, respectively). Moreover, the movement of bromo appendage from *para* position (**5c**, IC_{50} = 0.49 μM) to meta position (**5k**, IC_{50} = 0.41 μM) slightly enhanced the inhibitory action. On contrast, the *para* methoxy counterpart **5f** revealed a strong inhibitory influence (IC_{50} value of 0.28 μM) coming at the second order after the 4-nitro containing analogue (**5a**, IC_{50} = 0.22 μM).

Concerning benzothiazole-based thiazolidine-2,4-dione hybrids **8a**–**h**, it was obviously noted that replacement of the phenacyl moiety with benzothiazole motif improved the AR inhibitory effect by about twofold, except for the 4-nitro containing hybrid **8a** (IC_{50} = 1.98 μM) and 4-methoxy-grafted analogue **8f** (IC_{50} = 0.94 μM). It was detected that the incorporation of 4-chloro to the benzylidene moiety furnished the most efficient AR inhibitor within this study (IC_{50} value equals 0.16 μM) followed by the 4-bromo hybrid **8c** (IC_{50} = 0.21 μM). Thereafter, the other substitution pattern provided potent inhibition in the following order 3,4,5-trimethoxy hybrid **8g**, 4-methyl derivative **8e**, 4-fluoro analogue **8d**, and 3,4-dimethoxy derivative **8h** displaying IC_{50} values of 0.27, 0.29, 0.33, and 0.45 μM, respectively. Strikingly, it was deduced that the presence of 4-nitro **8a** or 4-methoxy **8e** on benzylidene moiety exerted negative influence on the inhibitory potency providing the least potent AR inhibitors within this study (IC_{50} values of 1.98 and 0.94 μM, respectively). Notably, it was deduced that the presence of methoxy substitutions on benzylidene moiety had an observable influence on the inhibitory potencies, where number of methoxy groups was directly proportional to the inhibitory activity; compound **8g** (IC_{50} of 0.27 μM) with three methoxy groups showed better activity than the two methoxy groups-appended derivative **8h** (IC_{50} of 0.45 μM) and the one methoxy-affixed analogue **8f** (IC_{50} of 0.94 μM), which possessed the least activity. Furthermore, the hybrid **8e** possessing a *para* methyl instead of methoxy functionality established a remarkable increment in its activity with IC_{50} of 0.29 μM.

Collectively, the introduction of 4-chloro, 4-bromo, or 3,4,5-trimethoxy substituents to the benzylidene moiety along with benzothiazole scaffold resulted in potent AR inhibitors. Besides, applying 4-nitro or 4-methoxy functionalities to the benzylidene moiety parallel with 4-nitro phenacyl group led to efficient AR inhibitors. Generally, the inferred SAR insights for the tested thiazolidine-2,4-dione hybrids can be employed for additional manipulations to develop more potent and safe AR inhibitors for the management of long-term diabetic complications.

Analysis of kinetic parameters for determination of 8b inhibition mode

The most potent AR inhibitor **8b** was selected for this study, the analysis of K_M and V_{max} of AR enzyme alone and with different concentrations of **8b** showed that at 0.5 IC_{50}, the compound led to significant reduction in V_{max} and slight reduction in K_m. In contrary, the K_m and V_{max} have been decreased significantly at concentrations equal to IC_{50} and double of IC_{50} with approximately fixed slope values, which is a unique pattern of non-competitive inhibitors, where K_M and V_{max} were reduced when the concentration of the inhibitor increased as shown in Figure 2. These findings indicate that the rationale design of **8b** was successful to produce similar compounds as the reported inhibitors.

Investigation of in vivo hypoglycaemic impact of the hybrid 8b

Streptozotocin (STZ)-induced diabetes is a widely used model to assess the hypoglycaemic effect of compounds. Since compound **8b** showed very comparable AR inhibitory activity to Epalrestat, its potential to decrease BG level *in vivo* was assessed using two doses (5 mg/kg and 50 mg/kg). In case of the lower dose, the BG level was reduced from 399.8 mg/dL (STZ group) to 362.333 mg/dL, while in the higher dose, it was decreased to 240 mg/dL after six weeks of treatment as depicted in Figure 3. This result highlighted that beside the observed *in vitro* AR inhibitory activity of the hybrid **8b**, it also has pronounced hypoglycaemic effect in dose-dependent manner as demonstrated in the experimental animals. This could be attributed due to the ability of thiazolidinedione to regulate other molecular targets associated

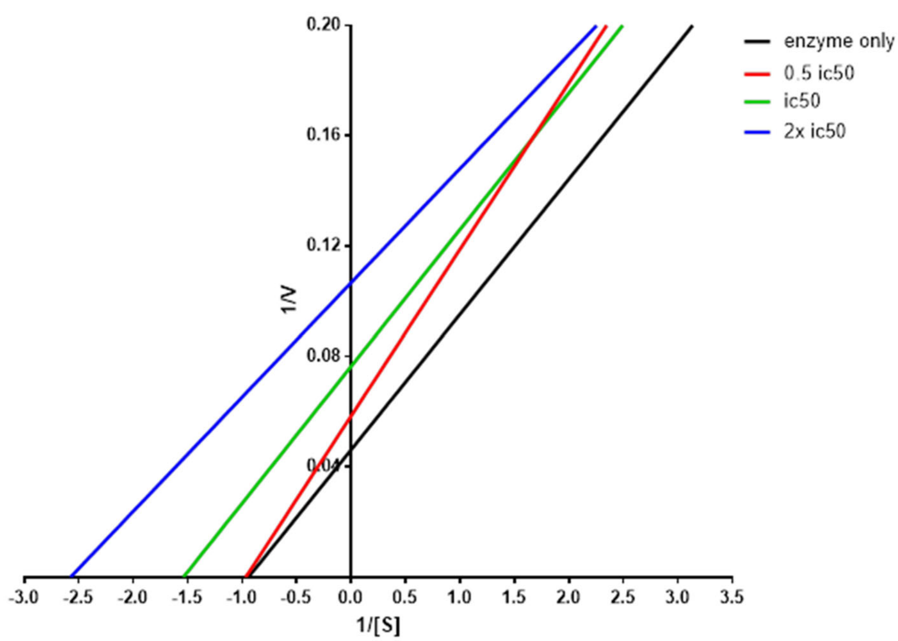

Figure 2. Lineweaver–Burk plot showing kinetics of aldose reductase in the absence and presence of different concentrations of **8b**.

with diabetes such as peroxisome proliferator-activated receptor gamma (PPAR-γ).[38]

Target fishing and molecular docking study of the most efficient hybrid 8b

Molecular docking tools have been used routinely in assessing the binding mode of bioactive compounds to explain their ability to inhibit several molecular targets[39–47]. So, taking into consideration the results of the kinetic study of compound **8b** and its observed hypoglycaemic effect *in vivo*, target fishing was used to identify potential pharmacological targets using Pharmmaper server. This server used preprepared pharmacophore model to identify molecular features in the compound of interest, then fit score is calculated and converted to *z*-score, which is modified fit score that takes statistic factor in consideration where the positive value indicates high significance of the target. After pharmacophore-based screening, AR, PPAR-γ, and glycogen synthase kinase-3 (GSK-3) emerged as the most relevant targets to diabetes with *z*-scores, 1.15, 0.54, and 0.6, respectively. Benzothiazole ring and thiazolidinedione moiety were highlighted as important pharmacophore in case of all the three enzymes. This could be explained in the light of the alignment of molecular features in compound **8b** with the pharmacophore model generated for aldose, reductase PPAR-γ and GSK-3 inhibitors as shown in Figure 2(S) and Table 1S. This finding agrees with previous studies reporting the ability of this class of compounds to inhibit these targets and could support the observed hypoglycaemic effect of compound **8b**[48–50].

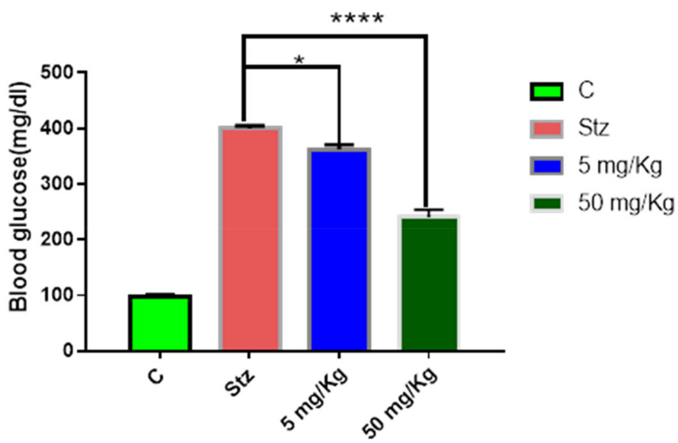

Figure 3. *In vivo* hypoglycaemic effect of compound **8b** in STZ-induced diabetes model after 6 weeks of treatment. Data shown are averages of six independent experiments $*p > 0.05$ and $****p > 0.0001$.

Molecular docking of compound **8b** at AR active site showed that it was able to bind to the same site of the reported non-competitive AR inhibitors. Also, it exerted remarkable binding energy −11.3 kcal/mol in comparison to −12 kcal/mol of the co-crystallised ligand. Since the co-crystallised ligand is one of the AR carboxylic acid inhibitors, it was able to exert several hydrogen bonds with Tyr48, HIS110, and TRP111 through its carboxylic acid moiety, also several hydrophobic interactions were observed with TRP20, TRP111; moreover, the trifluoro-benzothiazole ring was able to access the secondary hydrophobic pocket and formed hydrophobic interaction with Leu303A and PHE122.

Interestingly, compound **8b** best pose was aligned to the co-crystallised ligand, hence, it was able to reproduce most of these interaction to some extent, which explains its excellent binding affinity. Still, instead of the carboxylic group in the co-crystallised ligand, the thiazolidinedione ring formed hydrogen bonds with

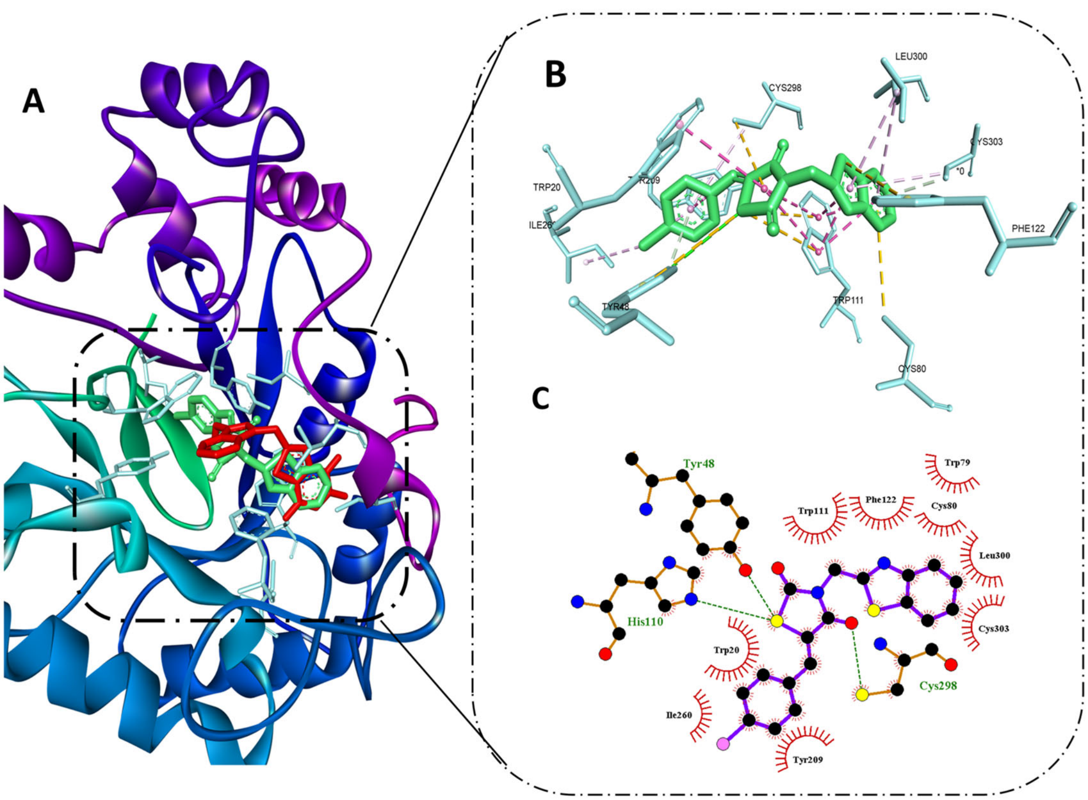

Figure 4. Molecular docking of **8b** in the active site of aldose reductase PDB: 3g5e. (A) Compound **8b** (green) aligned with the co-crystallised ligand (red). (B) 3D binding interaction of the hybrid **8b** with active site residues of aldose reductase. (C) 2D interaction of compound **8b** with active site residues of aldose reductase.

Table 2. Calculated parameters for Lipinski's rule and Veber's standards for the hybrids **5a**, **5f**, **8b**, **8c**, **8e**, and **8g**.

Comp.	Mwt[a]	*n*HBA[b]	*n*HBD[c]	Log*P*[d]	*n*Vs[e]	*n*RB[f]	TPSA[g]	% ABS[h]
Lipinski[i]	≤500	≤10	≤5	≤5	≤1	–	–	–
Veber[j]	–	–	–	–	–	≤10	≤140	–
5a	413.36	10	0	3.92	0	6	146.09	58.59
5f	398.39	8	0	3.94	0	6	109.50	71.22
8b	386.88	4	0	5.38	1	3	50.27	91.65
8c	431.33	4	0	5.59	1	3	50.27	91.65
8e	366.46	4	0	5.09	1	3	50.27	91.65
8g	442.51	7	0	4.15	0	6	77.96	82.10
Epalrestat	319.40	4	1	2.76	0	4	89.70	78.05

[a]Molecular weight.
[b]Number of hydrogen bond acceptors.
[c]Number of hydrogen bond donors.
[d]Lipophilicity (O/W).
[e]Number of Lipinski rule violations.
[f]Number of rotatable bonds.
[g]Topological polar surface area.
[h]Percentage of oral absorption.
[i]Reference values of Lipinski.
[j]Reference values of Veber.

TYR48, HIS110, and CYS298 maintaining the ability to halt the catalytic activity of the enzyme.

In addition, it formed hydrophobic interactions with amino acid residues in the backbone such as TRP20, and TRP111, while the benzothiazole ring demonstrated hydrophobic interactions with PHE122, LEU300, and CYS303 in the second selectivity hydrophobic site, which is in agreement to previous reports indicating that planar aromatic ring could improve the selectivity by accessing such hydrophobic pocket[51]. Finally, the benzylidene moiety interacted with TRP20, TYR209, ILE260, and CYS298 as shown in Figure 4. These binding interactions infer the importance of thiazolidinedione and benzothiazole moiety as assumed previously in the predicted pharmacophore model and previous reports showing their important role in achieving good AR inhibitory activity[52,53].

In silico prediction of physicochemical properties and pharmacokinetic profile

Lipinski's rule and Veber's parameters calculation

The oral bioavailability is one of the most important criteria in design and discovery of therapeutically active molecules[54]. Therefore, to predict the oral bioavailability and drug-likeness features for a candidate, Lipinski formulated "Rule of Five" using some main molecular descriptors like molecular weight, partition coefficient (log*P*), counts of hydrogen bond donors and acceptors[55]. Later, Veber added additional descriptors affecting drug oral bioavailability such as topological polar surface area (TPSA) and rotatable bonds numbers (nRB)[56]. The assessment of compliance of the most potent hybrids **5a**, **5f**, **8b**, **8c**, **8e**, and **8g** to Lipinski's rule and Veber's standard[57] revealed that all the tested compounds can serve as successful drug candidates where hybrids **5a**, **5f**, and **8g** are completely in agreement with Lipinski's rule with no violations, while compounds **8b**, **8c**, and **8e** displayed one violation (Log $P > 5$) as shown in Table 2. Concerning Veber's measures, the number of rotatable bonds of the tested hybrids was ≤10, exhibiting accepted molecular flexibility with subsequent good permeability and efficient oral bioavailability. Moreover, TPSA value of all the tested hybrids was in accordance with Veber's standards (TPSA < 140 Å^2) except for compound **5a** (TPSA (146.09) $>$140 Å^2). These TPSA assessments are used to estimate of oral absorption % (%ABS) theoretically applying the equation: %ABS $= 109 - (0.345$ TPSA$)$[58]. The hybrids **8b**, **8c**, and **8e** had % ABS of 91.65%, as well compound **5g** displayed % ABS of 82.10%, which may potentially allow better passive oral absorption relative to Epalrestat reference drug (78.05%). Based on these findings, it could be proposed that the hybrids **8b**, **8c**, **8e**, and **8g** had reasonable drug-likeness with good physicochemical characteristics and may be served as good orally active antidiabetic candidates.

Table 3. ADMET profile for the active hybrids **5a**, **5f**, **8b**, **8c**, **8e**, and **8g**.

Comp.	HIA	Caco2	MDCK	BBB	CYP3A4 inhibition	PgP inhibition	Carcinogenicity
5a	77.05	0.79	1.98	0.10	Non	Inhibitor	Negative
5f	94.80	0.99	1.03	0.21	Inhibitor	Inhibitor	Negative
8b	98.38	37.30	0.55	1.74	Non	Inhibitor	Negative
8c	97.94	41.54	0.02	1.86	Non	Inhibitor	Positive
8e	99.08	25.04	0.87	1.65	Non	Inhibitor	Negative
8g	100.00	23.56	0.26	0.35	Inhibitor	Inhibitor	Negative
Epalrestat	99.52	21.44	99.45	0.18	Non	Inhibitor	Negative

HIA: human intestinal absorption (%); Caco2: permeability through cells derived from human colon adenocarcinoma (nm/s); MDCK: permeability through Madin-Darby canine kidney cells (nm/s); tool for rapid permeability; BBB: blood–brain barrier penetration; CYP3A4: cytochrome P450 3A4; PgP: P-glycoprotein.

ADMET analysis

Calculation of the pharmacokinetic parameters (ADMET) is a significant step in early stage drug discovery for improvement of both drug efficacy and safety profile, in addition to avoidance of therapeutic agent failure as an effective clinical candidate[57]. Thus, ADMET profile of the most active hybrids **5a**, **5f**, **8b**, **8c**, **8e**, and **8g** was calculated theoretically using online Pre-ADMET server.

As shown in Table 3, the obtained calculations stated that all tested hybrids are predicted to have negative carcinogenic activities like reference drug except compound **8c**, which is predicted to be positive carcinogen. All compounds exerted excellent intestinal absorption with HIA values ranging 77.0–100%, displaying their potency as orally active drugs. They also showed medium CNS penetration (BBB values ranged 0.1–1.86) and low cellular permeability in MDCK cell model (MDCK < 25 nm/s). Besides, compound **5a** and **5f** showed low cellular permeability in CaCo2 cell model (CaCo2 values $<$4 nm/s); however, the hybrids **8b**, **8c**, **8e**, and **8g** displayed medium permeability with CaCo2 values ranging from 23.56 to 41.54 nm/s. Moreover, hybrids **5a**, **8b**, **8c**, and **8e** are not predicted to be involved in drug–drug interactions as they cannot inhibit CYP3A4 enzyme, in contrast to the positive control and the analogues **5f** and **8g**, which have CYP3A4 inhibitory action. Similarly, as the reference drug, all the assessed hybrids are inhibitors to P-glycoprotein (PgP); hence, it was anticipated to enhance bioavailability of the co-administered drugs.

Conclusions

Molecular hybridisation approach was exploited to design two series of 2,4-TZD hybrids **5a**–**k** and **8a**–**h** appending to either benzothiazole scaffold or *para* nitro phenacyl moiety, followed by their synthesis utilising different synthetic methodologies and spectral analyses for all analogues. After that, all the prepared analogues were assessed for their *in vitro* AR inhibitory effect. Interestingly, the majority of all derivatives displayed potential inhibitory impact at sub-micromolar level comparable to the positive control (Epalrestat). Noteworthy, the benzothiazole-tethered 2,4-TZD hybrid **8b** stood out as the most potent AR inhibitor within this study (**8b**, $IC_{50} = 0.16$ μM; **Epalrestat**, $IC_{50} = 0.10$ μM). Moreover, it was able to reduce BG level in STZ-induced diabetic animal model at 50 mg/kg dose from 399.8 mg/dL to 240 mg/dL. Furthermore, diverse *in silico* calculations suggested that these candidates possess drug-likeness characters and acceptable pharmacokinetics as non-competitive AR inhibitors. Also, target fishing shows that compound **8b** has several pharmacophoric features similar to the inhibitors of AR, PPAR-γ, and GSK-3 AIs. Molecular docking study displayed that hybrid **8b** can bind to AR active site in a similar pattern as the reported AR inhibitors. Collectively, the new 2,4-TZD hybrids could be used as candidates for development of more efficient and selective AR inhibitors for management of serious diabetic complications.

Experimental

Chemistry

General

Melting points (°C) were determined using Stuart apparatus (SMP 30) and are uncorrected. IR spectra (KBr) were recorded on FT-IR 200 spectrophotometer ($\acute{\upsilon}$ cm^{-1}), Faculty of Pharmacy, Mansoura University, Mansoura, Egypt. ^{1}H NMR and ^{13}C NMR spectra were measured in DMSO-d$_6$ at ^{1}H NMR (400 MHz), ^{13}C NMR (100 MHz) using TMS as an internal standard, at NMR Unit, Faculty of Pharmacy, Mansoura University, Mansoura, Egypt. The following abbreviations are used as follows: s, singlet; d, doublet; t, triplet; m, multiplet; br, broad, chemical shift (δ ppm). Mass spectra were carried out on direct inlet part to mass analyser utilising Thermo Scientific GCMS model ISQ at the Regional Center for Mycology and Biotechnology (RCMB), Al-Azhar University, Assiut, Egypt. All the chemicals and reagents used were purchased from Aldrich Chemicals Co. (Milwaukee, WI) and commercial sources. Reaction times were determined using TLC on silica gel plates 60F245 E. Merck, using hexane/EtOAc (1:1) as eluting system and the spots were visualised by UV (366–245 nm).

The key precursors, thiazolidinedione (**2**), 1,3-thiazolidine-2,4-dione derivative (**4a**–**l**) and benzothiazole chloride **7** could be easily prepared according to the previously described literature procedures[33,59].

General procedure for synthesis of (Z)-5-(4 or 3-substitutedbenzylidene)-3-(2-(4-nitrophenyl)-2-oxoethyl)thiazolidine-2,4-dione (5a–k)

The potassium salts **4a**–**k** (0.30 mmol, 1 equiv.) and 2-bromo-4′-nitroacetophenone 95% (0.30 mmol, 1 equiv.) were mixed together in a round-bottomed flask along with 10 mL dry DMF. Thereafter, the reaction mixture was stirred at room temperature and the reaction progress was monitored by TLC. Twelve hours later, the reaction was stopped, and the reaction mixture was quenched with water. The separated solid was filtrated off and crystallised from ethanol to produce the corresponding nitro-phenacyl-based thiazolidine-2,4-dione hybrids in pure form **5a**–**k**.

(Z)-5-(4-nitrobenzylidene)-3-(2-(4-nitrophenyl)-2-oxoethyl)thiazolidine-2,4-dione (5a). Pale yellow solid; (0.095 g, 77%). M.p. 204–206 °C. IR (νmax/cm^{-1}): 3075, 2982 (CH), 1748, 1691 (C=O), 1609, 1525, 1220. ^{1}H NMR (400 MHz, DMSO-*d$_6$*) δ 8.42 (d, J = 8.8 Hz, 2H), 8.39 (d, J = 8.8 Hz, 2H), 8.35 (d, J = 8.6 Hz, 2H), 8.16 (s, 1H), 7.96 (d, J = 8.6 Hz, 2H), 5.49 (s, 2H). ^{13}C NMR (101 MHz, DMSO-*d$_6$*) δ 191.4, 167.0, 165.3, 151.1, 148.3, 139.5, 138.7, 132.0, 131.7, 130.4, 125.5, 124.8, 124.5, 48.9. MS *m/z* (%): 413.9 (M$^+$, 48.61).

(Z)-5-(4-chlorobenzylidene)-3-(2-(4-nitrophenyl)-2-oxoethyl)thiazolidine-2,4-dione (5b). Yellow solid; (0.105 g, 88%). M.p. 260–262 °C. IR (νmax/cm^{-1}): 3111, 2975 (CH), 1738, 1684 (C=O), 1601, 1526, 1221. ^{1}H NMR (400 MHz, DMSO-*d$_6$*) δ 8.42 (d, J = 8.8 Hz, 2H), 8.34 (d, J = 8.8 Hz, 2H), 8.04 (s, 1H), 7.72 (d, J = 8.5 Hz, 2H), 7.66 (d, J = 8.5 Hz, 2H), 5.46 (s, 2H). ^{13}C NMR (101 MHz, DMSO-*d$_6$*) δ 192.1, 167.3, 165.5, 151.5, 139.0, 136.6, 134.5, 133.3, 132.4, 130.4, 130.0, 124.5, 122.0, 48.7. MS *m/z* (%): 402.7 (M$^+$, 17.58).

(Z)-5-(4-bromobenzylidene)-3-(2-(4-nitrophenyl)-2-oxoethyl)thiazolidine-2,4-dione (5c). Yellow solid; (0.100 g, 75%). M.p. 241–243 °C. IR (νmax/cm^{-1}): 3076, 2969 (CH), 1748, 1696 (C=O), 1605, 1527, 1216. ^{1}H NMR (400 MHz, DMSO-*d$_6$*) δ 8.42 (d, J = 8.7 Hz, 2H), 8.34 (d, J = 8.7 Hz, 2H), 8.02 (s, 1H), 7.80 (d, J = 8.3 Hz, 2H), 7.65 (d, J = 8.3 Hz, 2H), 5.46 (s, 2H). ^{13}C NMR (101 MHz, DMSO-*d$_6$*) δ 191.5, 167.2, 165.5, 151.1, 138.8, 136.0, 133.3, 132.4, 132.2, 130.4, 130.0, 124.5, 122.0, 48.8. MS *m/z* (%): 447.1 (M$^+$, 22.32).

(Z)-5-(4-fluorobenzylidene)-3-(2-(4-nitrophenyl)-2-oxoethyl)thiazolidine-2,4-dione (5d). White solid; (0.098 g, 85%). M.p. 201–203 °C. IR (νmax/cm^{-1}): 3111, 2982 (CH), 1748, 1691 (C=O), 1596, 1520, 1151. ^{1}H NMR (400 MHz, DMSO-*d$_6$*) δ 8.42 (d, J = 8.4 Hz, 2H), 8.34 (d, J = 8.4 Hz, 2H), 8.05 (s, 1H), 7.78 (d, J = 7.0 Hz, 2H), 7.44 (d, J = 7.0 Hz, 2H), 5.46 (s, 2H). ^{13}C NMR (101 MHz, DMSO-*d$_6$*) δ 191.5, 167.3, 165.6, 151.1, 138.8, 133.5, 133.3, 130.4, 129.9, 124.5, 120.9, 117.2, 117.0, 48.7. MS *m/z* (%): 386.2 (M$^+$, 24.88).

(Z)-5-(4-methylbenzylidene)-3-(2-(4-nitrophenyl)-2-oxoethyl)thiazolidine-2,4-dione (5e). Yellow solid; (0.08 g, 70%). M.p. 239–241 °C. IR (νmax/cm^{-1}): 3076, 2969 (CH), 1732, 1678 (C=O), 1596, 1535, 1222. ^{1}H NMR (400 MHz, DMSO-*d$_6$*) δ 8.42 (d, J = 8.8 Hz, 2H), 8.35 (d, J = 8.8 Hz, 2H), 8.00 (s, 1H), 7.60 (d, J = 8.2 Hz, 2H), 7.41 (d, J = 8.2 Hz, 2H), 5.45 (s, 2H), 2.40 (s, 3H). ^{13}C NMR (101 MHz, DMSO-*d$_6$*) δ 191.6, 167.8, 165.6, 162.3, 151.7, 136.8, 132.3, 130.9, 130.3, 125.2, 124.5, 118.4, 114.6, 48.7, 21.6. MS *m/z* (%): 382.0 (M$^+$, 40.09).

(Z)-5-(4-methoxybenzylidene)-3-(2-(4-nitrophenyl)-2-oxoethyl)thiazolidine-2,4-dione *(5f).* Pale yellow solid; (0.107 g, 90%). M.p. IR (νmax/cm^{-1}): 3068, 2968 (CH), 1742, 1680 (C=O), 1598, 1520, 1325. ^{1}H NMR (400 MHz, DMSO-*d$_6$*) δ 8.42 (d, J = 8.8 Hz, 2H), 8.34 (d, J = 8.8 Hz, 2H), 7.99 (s, 1H), 7.67 (d, J = 8.8 Hz, 2H), 7.16 (d, J = 8.8 Hz, 2H), 5.43 (s, 2H), 3.87 (s, 3H). ^{13}C NMR (101 MHz, DMSO-*d$_6$*) δ 191.6, 167.5, 165.7, 161.9, 151.1, 138.8, 134.6, 132.96, 130.4, 125.7, 124.5, 117.9, 115.6, 56.1, 48.6. MS *m/z* (%): 398.05 (M$^+$, 25.10).

(Z)-3-(2-(4-nitrophenyl)-2-oxoethyl)-5-(3,4,5-trimethoxybenzylidene)thiazolidine-2,4-dione (5g). Yellow solid; (0.110 g, 80%). M.p. 184–186 °C. IR (νmax/cm^{-1}): 3070, 2969 (CH), 1740, 1680 (C=O), 1596, 1535, 1220. ^{1}H NMR (400 MHz, DMSO-*d$_6$*) δ 8.42 (d, J = 8.6 Hz, 2H), 8.34 (d, J = 8.6 Hz, 2H), 7.98 (s, 1H), 7.01 (s, 2H), 5.46 (s, 2H), 3.87 (s, 6H), 3.76 (s, 3H). ^{13}C NMR (101 MHz, DMSO-*d$_6$*) δ 191.6, 167.4, 165.6, 153.8, 151.1, 140.3, 138.8, 134.8, 130.4, 128.8, 124.5, 120.1, 108.3, 60.7, 56.5, 48.7. MS *m/z* (%): 458.13 (M$^+$, 79.45).

(Z)-5-(3-nitrobenzylidene)-3-(2-(4-nitrophenyl)-2-oxoethyl)thiazolidine-2,4-dione (5h). Yellow solid; (0.085 g, 69%). M.p. 196–198 °C. IR (νmax/cm^{-1}): 3080, 2980 (CH), 1751, 1693 (C=O), 1609, 1521, 1224. ^{1}H NMR (400 MHz, DMSO-*d$_6$*) δ 8.47–8.31 (m, 6H), 8.15 (s, 1H), 7.96 (d, J = 7.2 Hz, 2H), 5.48 (s, 2H). ^{13}C NMR (101 MHz, DMSO-d_6) δ 191.7, 167.5, 165.6, 149.4, 147.8, 138.9, 136.2, 133.3, 133.1, 129.9, 129.4, 128.7, 124.5, 124.2, 123.0, 48.7. MS m/z (%): 413.3 (M^+, 35.75).

(Z)-5-(3-bromobenzylidene)-3-(2-(4-nitrophenyl)-2-oxoethyl)thiazolidine-2,4-dione (5k). Yellow solid; (0.101, 75%). M.p. 179–181 °C. IR (νmax/cm^{-1}): 3108, 2985 (CH), 1752, 1692 (C=O), 1601, 1520, 1151. ^{1}H NMR (400 MHz, DMSO-d_6) δ 8.42 (d, J = 8.8 Hz, 2H), 8.35 (d, J = 8.8 Hz, 2H), 8.04 (s, 1H), 7.93 (s, 1H), 7.75 (d, J = 7.8 Hz, 1H), 7.68 (d, J = 7.8 Hz, 1H), 7.55 (t, J = 7.9 Hz, 1H), 5.47 (s, 2H). ^{13}C NMR (101 MHz, DMSO-d_6) δ 191.5, 167.1, 165.4, 151.1, 138.7, 135.7, 133.8, 133.7, 132.9, 131.9, 130.4, 128.7, 124.5, 123.0, 123.0, 48.8. MS m/z (%): 447.1 (M^+, 13.52).

General procedure for the preparation of (Z)-3-(benzo[d]thiazol-2-ylmethyl)-5-(4-subtitutedbenzylidene)thiazolidine-2,4-dione (8a–h)

The potassium salts **4a**–**g**, **4l** (0.32 mmol, 1 equiv.) and 2-chloromethyl-1,3-benzothiazole **7** (0.32 mmol, 1 equiv.) were added together in a round-bottomed flask along with 10 mL dry DMF. After that, the reaction mixture was heated under reflux and the reaction progress was monitored by TLC. After 12 h, the reaction was stopped, and the reaction mixture was quenched with water. The separated solid was filtrated off and crystallised from ethanol to obtain the corresponding benzothiazole-based thiazolidine-2,4-dione hybrids in pure form **8a**–**h**.

(Z)-3-(benzo[d]thiazol-2-ylmethyl)-5-(4-nitrobenzylidene)thiazolidine-2,4-dione *(8a)*. Yellow solid; (0.095 g, 74%). M.p. 190–192 °C. IR (νmax/cm^{-1}): 3026, 2937 (CH), 1745, 1680 (C=O), 1608, 1580, 1145. ^{1}H NMR (400 MHz, DMSO-d_6) δ 8.38 (d, J = 7.9 Hz, 2H), 8.17 (s, 1H), 8.13 (d, J = 7.8 Hz, 1H), 7.99 (d, J = 7.8 Hz, 1H), 7.95 (d, J = 7.9 Hz, 2H), 7.60–7.50 (m, 2H), 5.36 (s, 2H). ^{13}C NMR (101 MHz, DMSO-d_6) δ 166.9, 165.2, 164.9, 152.4, 148.3, 139.5, 135.4, 132.0, 131.6, 131.1, 126.9, 126.1, 124.8, 123.2, 122.9, 43.4. MS m/z (%): 397.4 (M^+, 22.5).

(Z)-3-(benzo[d]thiazol-2-ylmethyl)-5-(4-chlorobenzylidene)thiazolidine-2,4-dione (8b). White solid; (0.082 g, 70%). M.p. 159–161 °C. IR (νmax/cm^{-1}): 3022, 2930 (CH), 1738, 1678 (C=O), 1605, 1585, 1130.^{1}H NMR (400 MHz, DMSO-d_6) δ 8.12 (d, J = 7.8 Hz, 1H), 8.05 (s, 1H), 7.99 (d, J = 7.8 Hz, 1H), 7.71 (d, J = 8.4 Hz, 2H), 7.65 (d, J = 8.4 Hz, 2H), 7.60–7.50 (m, 2H), 5.34 (s, 2H). ^{13}C NMR (101 MHz, DMSO-d_6) δ 167.2, 165.4, 165.1, 152.5, 136.0, 135.3, 133.3, 132.4, 132.2, 130.0, 126.9, 126.0, 123.2, 122.9, 122.0, 43.3. MS m/z (%): 386.6 (M^+, 14.20).

(Z)-3-(benzo[d]thiazol-2-ylmethyl)-5-(4-bromobenzylidene)thiazolidine-2,4-dione (8c). Pale yellow solid; (0.085 g, 66%). M.p. 174–176 °C. IR (νmax/cm^{-1}): 3027, 2930 (CH), 1740, 1683 (C=O), 1607, 1580, 1132. ^{1}H NMR (400 MHz, $CDCl_3$) δ 8.07 (d, J = 8.2 Hz, 1H), 7.93 (s, 1H), 7.88 (d, J = 8.2 Hz, 1H), 7.65 (d, J = 8.4 Hz, 2H), 7.51 (t, J = 7.7 Hz, 1H), 7.46–7.39 (m, 3H), 5.38 (s, 2H). ^{13}C NMR (101 MHz, DMSO-d_6) δ 167.4, 165.4, 165.2, 152.4, 135.4, 133.5, 133.4, 130.0, 126.9, 126.0, 123.2, 122.9, 120.9, 117.3, 117.1, 43.1. MS m/z (%): 431.1 (M^+, 30.1).

(Z)-3-(benzo[d]thiazol-2-ylmethyl)-5-(4-fluorobenzylidene)thiazolidine-2,4-dione (8d). Pale yellow solid; (0.079 g, 71%). M.p. 190–192 °C. IR (νmax/cm^{-1}): 3020, 2930 (CH), 1738, 1685 (C=O), 1607, 1580, 1130.^{1}H NMR (400 MHz, DMSO-d_6) δ 8.12 (d, J = 7.9 Hz, 1H), 8.07 (s, 1H), 7.99 (d, J = 7.9 Hz, 1H), 7.81–7.73 (m, 2H), 7.55–7.42 (m, 4H), 5.34 (s, 2H). ^{13}C NMR (101 MHz, DMSO-d_6) δ 167.3, 165.5, 165.2, 152.5, 135.3, 133.5, 133.3, 133.2, 126.9, 126.1, 123.2, 122.9, 120.9, 117.2, 117.0, 43.3. MS m/z (%): 370.93 (M^+, 45.49).

(Z)-3-(benzo[d]thiazol-2-ylmethyl)-5-(4-methylbenzylidene)thiazolidine-2,4-dione (8e). Off-white solid; (0.090 g, 82%). M.p. 163–165 °C. IR (νmax/cm^{-1}): 3025, 2940 (CH), 1740, 1691 (C=O), 1607, 1575, 1145. ^{1}H NMR (400 MHz, DMSO-d_6) δ 8.12 (d, J = 7.4 Hz, 1H), 8.00 (s, 1H), 7.97 (d, J = 7.4 Hz, 1H), 7.58 (d, J = 7.3 Hz, 2H), 7.56–7.44 (m, 2H), 7.40 (d, J = 7.3 Hz, 2H), 5.33 (s, 2H), 2.51 (s, 3H). ^{13}C NMR (101 MHz, DMSO-d_6) δ 167.5, 165.5, 165.3, 152.5, 141.8, 135.3, 134.7, 130.8, 130.7, 130.6, 126.9, 126.0, 123.2, 122.9, 119.9, 43.3, 21.6. MS m/z (%): 366.4 (M^+, 18.2).

(Z)-3-(benzo[d]thiazol-2-ylmethyl)-5-(4-methoxybenzylidene)thiazolidine-2,4-dione *(8f)*. Pale yellow solid; (0.085 g, 70%). M.p. IR (νmax/cm^{-1}): 3024, 2939 (CH), 1740, 1680 (C=O), 1610, 1580. ^{1}H NMR (400 MHz, DMSO) δ 8.10 (d, J = 7.6 Hz, 1H), 7.99 (s, 1H), 7.98 (d, J = 7.6 Hz, 1H), 7.65 (d, J = 8.4 Hz, 2H), 7.55–7.44 (m, 2H), 7.14 (d, J = 8.5 Hz, 2H), 5.32 (s, 2H), 3.85 (s, 3H). ^{13}C NMR (101 MHz, DMSO-d_6) δ 167.5, 166.0, 165.4, 152.5, 135.3, 134.6, 133.0, 132.6, 132.3, 126.9, 126.0, 123.2, 122.9, 117.8, 115.5, 56.0, 43.2. MS m/z (%): 382.2 (M^+, 20.4).

(Z)-3-(benzo[d]thiazol-2-ylmethyl)-5-(3,4,5-trimethoxybenzylidene)thiazolidine-2,4-dione *(8g)*. Pale yellow solid; (0.066 g, 50%). M.p. 140–142 °C. IR (νmax/cm^{-1}): 3020, 2950 (CH), 1738, 1685 (C=O), 1607, 1580, 1200. ^{1}H NMR (400 MHz, DMSO-d_6) δ 8.12 (d, J = 7.9 Hz, 1H), 8.00 (s, 1H), 7.97 (d, J = 7.9 Hz, 1H), 7.60–7.50 (m, 2H), 7.01 (s, 2H), 5.34 (s, 2H), 3.86 (s, 6H), 3.76 (s, 3H). MS m/z (%): 442.3 (M^+, 22.92).

(Z)-3-(benzo[d]thiazol-2-ylmethyl)-5-(3,4-dimethoxybenzylidene)-thiazolidine-2,4-dione *(8h)*. Yellow solid; (0.080 g, 60%). M.p. 180–182 °C. IR (νmax/cm^{-1}): 3020, 2935 (CH), 1738, 1680 (C=O), 1609, 1585, 1140. ^{1}H NMR (400 MHz, DMSO-d_6) δ 8.12 (d, J = 7.8 Hz, 1H), 8.00 (s, 1H), 7.98 (d, J = 7.8 Hz, 1H), 7.60–7.50 (m, 2H), 7.28 (s, 2H), 7.17 (d, J = 8.8 Hz, 1H), 5.33 (s, 2H), 3.86 (s, 3H), 3.84 (s, 3H). ^{13}C NMR (101 MHz, DMSO-d_6) δ 167.5, 165.9, 165.5, 155.2, 152.5, 149.1, 136.3, 134.8, 132.9, 132.6, 129.4, 126.5, 126.0, 123.4, 122.2, 113.9, 113.4, 60.1, 56.5, 43.6. MS m/z (%): 412.3 (M^+, 25.2).

Biological evaluation of the synthesised compounds

In vitro enzyme inhibitory assay against human aldose reductase

Enzyme inhibitory assays for the synthesised compounds were carried out using AR activity assay kit (ab273276) according to the manufacturer instructions. From the obtained dose response curve, the concentration of the compounds inhibiting 50% of enzyme (IC_{50}) was calculated.

Kinetic study of inhibitory effect of 8b against aldose reductase

Since compound **8b** showed the best activity, it was subjected for kinetic study to determine its binding mode by determination of its effect on K_m and V_{max} of AR upon incubation with half IC_{50}, IC_{50}, and double IC_{50} of **8b**. The Michaelis–Menten equation was used to calculate both K_M and V_{max} using non-linear regression by the aid of GraphPad Prism 8.0 (La Jolla, CA) and data were presented using Lineweaver–Burk plot.

Effect of compound 8b in blood glucose level in diabetic mice

Twenty-four male mice with an average weight of 25.41 ± 2.13 g, were used in this study. Six mice/cage were housed at room temperature with 12 h dark/light cycle under standardised environmental conditions with free access to water and food till initiation of the experimental protocol. All animal experiments were done in agreement with ethical guidelines for animal experimentation. Animals in specific groups were injected I.P. with solution of STZ (Sigma, Carlsbad, CA), at final dosage of 40 mg/kg BW, freshly prepared in 0.1 mol/L citrate–phosphate buffer, pH 4.5 for five successive days, then BG was determined, and the mice with established hyperglycaemia (>300 mg/dL) were involved in the study. Mice were randomly assigned as six mice per group as follows: vehicle control group (group I), received the STZ injection only (group II), received 5 mg/kg of compound **8b** after STZ-induction (group III), and final group received 50 mg/kg after STZ-induction (group IV). After 6 weeks, fasting glucose levels were monitored and compared with initial glucose level. Statistical analysis was performed using one-way analysis of variance (ANOVA) using GraphPad Prism 8.0 (La Jolla, CA). A p value of less than 0.05 was considered significant. The mean and standard error of the mean were used to describe all of the obtained results. The research ethics committee at Kafrelsheikh University, Kafrelsheikh, Egypt examined and authorised the experiments (code number: KFS-IACUC/116/2023).

Molecular docking and ADME prediction studies

In silico tools were used to gain insights on potential mechanism of action of compound **8b** and to assess its ability **8b** to bind to AR. First, the 3D chemical structures of **8b** were submitted to Pharmmaper server (http://www.lilab-ecust.cn/pharmmapper/) and the top targets related to diabetes were chosen based on their *z*-score[60].

For molecular docking studies, the crystal structure of AR was obtained from PDB using the code: **3g5e**, which was subjected to protein repair and analysis[61,62]. Protein preparation module integrated in PyRx software was used to determine the active site coordinate, which was defined as X: 22, Y: −7, and Z: 23 and the grid box size was 22 × 22 × 32[63].

Compound **8b** 2D structure was prepared using Marvin sketch version 21.17.0, ChemAxon (https://www.chemaxon.com) and saved as mol files and converted to PDBQT using AutoDock tools embedded in PyRX. Autodock vina was chosen to perform molecular docking, using default parameters. The validation of PyRx was confirmed by redocking the co-crystallised ligand and the RMSD was shown to be no more than 1.5 Å (Figure 1S). The best ranked pose in terms of binding free energy (ΔG) was analysed by visualisation of the interaction with the active site using discovery studio visualiser 20.0[64]. The most active compounds in the biological assay were also submitted to PreADMET online server (https://preadmet.qsarhub.com/) to predict their Pharmacokinetic properties.

Acknowledgements

We are thankful to the Research supporting project number (RSPD2023R740), King Saud University, Riyadh, Saudi Arabia.

Disclosure statement

The authors declare no conflicts of interest.

Funding

Research supporting project number (RSPD2023R740), King Saud University, Riyadh, Saudi Arabia.

ORCID

Abdelrahman Hamdi http://orcid.org/0000-0002-0196-1976
Muhammad Yaseen http://orcid.org/0000-0002-2259-4589
Wafaa A. Ewes http://orcid.org/0000-0001-7690-2906
Mashooq Ahmad Bhat http://orcid.org/0000-0001-8426-4692
Noha I. Ziedan http://orcid.org/0000-0002-9522-2188
Hamed W. El-Shafey http://orcid.org/0000-0002-7848-8785
Ahmed A. B. Mohamed http://orcid.org/0000-0003-3912-1021
Mohamed R. Elnagar http://orcid.org/0000-0003-0434-2369
Abdullah Haikal http://orcid.org/0000-0003-2548-3507
Abdullah A. Elgazar http://orcid.org/0000-0002-5851-3306
Ahmed H. A. Abusabaa http://orcid.org/0009-0000-3770-4042
Kamal S. Abdelrahman http://orcid.org/0000-0002-2661-6159
Osama M. Soltan http://orcid.org/0000-0001-9738-2436
Mostafa M. Elbadawi http://orcid.org/0000-0002-9073-4176

References

1. Pasala VK, Gudipudi G, Sankeshi V, Basude M, Gundla R, Singh Jadav S, Srinivas B, Goud EY, Nareshkumar D. Design, synthesis and biological evaluation of selective hybrid coumarin-thiazolidinedione aldose reductase-II inhibitors as potential antidiabetics. Bioorg Chem. 2021;114:104970.
2. Imran M, Yar MS, Khan SA. Synthesis and antihyperglycemic activity of 2-(substituted phenyl)-3-{[4-(1-naphthyl)-1, 3-thiazol-2-yl] amino}-4-oxo-1, 3-thiazolidin-5-ylacetic acid derivatives. Acta Pol Pharm. 2009;66(1):51–56.
3. Sever B, Altıntop MD, Demir Y, Türkeş C, Özbaş K, Çiftçi GA, Beydemir Ş, Özdemir A. A new series of 2,4-thiazolidinediones endowed with potent aldose reductase inhibitory activity. Open Chem. 2021;19(1):347–357.
4. Singh Grewal A, Bhardwaj S, Pandita D, Lather V, Singh Sekhon B. Updates on aldose reductase inhibitors for management of diabetic complications and non-diabetic diseases. Mini Rev Med Chem. 2016;16(2):120–162.
5. Seltzer HS. Drug-induced hypoglycemia: a review of 1418 cases. Endocrinol Metab Clin N Am. 1989;18(1):163–183.
6. O Moore-Sullivan TM, Prins JB. Thiazolidinediones and type 2 diabetes: new drugs for an old disease. Med J Aust. 2002;176(8):381–386.
7. Lee AY, Chung SS. Contributions of polyol pathway to oxidative stress in diabetic cataract. FASEB J. 1999;13(1):23–30.
8. Bozdağ-Dündar O, Evcimen ND, Ceylan-Ünlüsoy M, Ertan R, Sarıkaya M. Some new thiazolyl thiazolidinedione derivatives as aldose reductase inhibitors. Med Chem Res. 2008;16(1):39–47.
9. Alexiou P, Pegklidou K, Chatzopoulou M, Nicolaou I, Demopoulos VJ. Aldose reductase enzyme and its implication to major health problems of the 21st century. Curr Med Chem. 2009;16(6):734–752.
10. Pfeifer MA, Schumer MP, Gelber DA. Aldose reductase inhibitors: the end of an era or the need for different trial designs? Diabetes. 1997;46(Suppl. 2):S82–S89.
11. Kador PF, Robison WG Jr, Kinoshita JH. The pharmacology of aldose reductase inhibitors. Annu Rev Pharmacol Toxicol. 1985;25:691–714.

12. Costantino L, Rastelli G, Gamberini MC, Barlocco D. Pharmacological approaches to the treatment of diabetic complications. Expert Opin Ther Pat. 2000;10(8):1245–1262.
13. Costantino L, Ferrari AM, Gamberini MC, Rastelli G. Nitrophenyl derivatives as aldose reductase inhibitors. Bioorg Med Chem. 2002;10(12):3923–3931.
14. Kousaxidis A, Kovacikova L, Nicolaou I, Stefek M, Geronikaki A. Non-acidic bifunctional benzothiazole-based thiazolidinones with antimicrobial and aldose reductase inhibitory activity as a promising therapeutic strategy for sepsis. Med Chem Res. 2021;30(10):1837–1848.
15. Kratky M, Sramel P, Bodo P, Prnova MS, Kovacikova L, Majekova M, Vinsova J, Stefek M. Novel rhodanine based inhibitors of aldose reductase of non-acidic nature with p-hydroxybenzylidene functional group. Eur J Med Chem. 2023;246:114922.
16. Bacha MM, Nadeem H, Zaib S, Sarwar S, Imran A, Rahman SU, Ali HS, Arif M, Iqbal J. Rhodanine-3-acetamide derivatives as aldose and aldehyde reductase inhibitors to treat diabetic complications: synthesis, biological evaluation, molecular docking and simulation studies. BMC Chem. 2021; 15(1):1–15.
17. Hotta N, Sakamoto N, Shigeta Y, Kikkawa R, Goto Y, Diabetic Neuropathy Study Group in Japan. Clinical investigation of Epalrestat, an aldose reductase inhibitor, on diabetic neuropathy in Japan: multicenter study. J Diabetes Complications. 1996;10(3):168–172.
18. Hotta N, Akanuma Y, Kawamori R, Matsuoka K, Oka Y, Shichiri M, Toyota T, Nakashima M, Yoshimura I, Sakamoto N, et al. Long-term clinical effects of Epalrestat, an aldose reductase inhibitor, on diabetic peripheral neuropathy: the 3-year, multicenter, comparative aldose reductase inhibitor-diabetes complications trial. Diabetes Care. 2006;29(7):1538–1544.
19. Terashima H, Hama K, Yamamoto R, Tsuboshima M, Kikkawa R, Hatanaka I, Shigeta Y. Effects of a new aldose reductase inhibitor on various tissues in vitro. J Pharmacol Exp Ther. 1984;229(1):226–230.
20. Das-Evcimen N, Sarıkaya M, Selen Gurkan-Alp A, Bozdag-Dundar O. Aldose reductase inhibitory potential of several thiazolyl-thiazolidine-2,4-diones. Lett Drug Des Discov. 2013; 10(5):415–419.
21. Bozdağ-Dündar O, Evranos B, Daş-Evcimen N, Sarıkaya M, Ertan R. Synthesis and aldose reductase inhibitory activity of some new chromonyl-2,4-thiazolidinediones. Eur J Med Chem. 2008;43(11):2412–2417.
22. Maccari R, Del Corso A, Giglio M, Moschini R, Mura U, Ottanà R. In vitro evaluation of 5-arylidene-2-thioxo-4-thiazolidinones active as aldose reductase inhibitors. Bioorg Med Chem Lett. 2011;21(1):200–203.
23. Ottanà R, Maccari R, Giglio M, Del Corso A, Cappiello M, Mura U, Cosconati S, Marinelli L, Novellino E, Sartini S, et al. Identification of 5-arylidene-4-thiazolidinone derivatives endowed with dual activity as aldose reductase inhibitors and antioxidant agents for the treatment of diabetic complications. Eur J Med Chem. 2011;46(7):2797–2806.
24. Mylari BL, Larson ER, Beyer TA, Zembrowski WJ, Aldinger CE, Dee MF, Siegel TW, Singleton DH. Novel, potent aldose reductase inhibitors: 3,4-dihydro-4-oxo-3-[[5-(trifluoromethyl)-2-benzothiazolyl] methyl]-1-phthalazineacetic acid (Zopolrestat) and congeners. J Med Chem. 1991;34(1): 108–122.
25. Imran A, Shehzad MT, Shah SJA, Al Adhami T, Laws M, Rahman KM, Alharthy RD, Khan IA, Shafiq Z, Iqbal J. Development and exploration of novel substituted thiosemicarbazones as inhibitors of aldose reductase via in vitro analysis and computational study. Sci Rep. 2022;12(1):5734.
26. Aotsuka T, Abe N, Fukushima K, Ashizawa N, Yoshida M. Benzothiazol-2-ylcarboxylic acids with diverse spacers: a novel class of potent, orally active aldose reductase inhibitors. Bioorg Med Chem Lett. 1997;7(13):1677–1682.
27. Kotani T, Nagaki Y, Ishii A, Konishi Y, Yago H, Suehiro S, Okukado N, Okamoto K. Highly selective aldose reductase inhibitors. 3. Structural diversity of 3-(arylmethyl)-2,4,5-trioxoimidazolidine-1-acetic acids. J Med Chem. 1997;40(5): 684–694.
28. Kotani T, Ishii A, Nagaki Y, Toyomaki Y, Yago H, Suehiro S, Okukado N, Okamoto K. Highly selective aldose reductase inhibitors. II. Optimization of the aryl part of 3-(arylmethyl)-2,4,5-trioxoimidazolidine-1-acetic acids. Chem Pharm Bull. 1997;45(2):297–304.
29. Zaher N, Nicolaou I, Demopoulos VJ. Pyrrolylbenzothiazole derivatives as aldose reductase inhibitors. J Enzyme Inhib Med Chem. 2002;17(2):131–135.
30. Kousaxidis A, Petrou A, Rouvim P, Bodo P, Stefek M, Nicolaou I, Geronikaki A. A molecular hybridization approach for the design of selective aldose reductase (ALR2) inhibitors and exploration of their activities against protein tyrosine phosphatase 1B (PTP1B). J Mol Struct. 2023;1271:134116.
31. Hussain S, Parveen S, Qin X, Hao X, Zhang S, Chen X, Zhu C, Ma B. Novel synthesis of nitro-quinoxalinone derivatives as aldose reductase inhibitors. Bioorg Med Chem Lett. 2014; 24(9):2086–2089.
32. Ishii A, Kotani T, Nagaki Y, Shibayama Y, Toyomaki Y, Okukado N, Ienaga K, Okamoto K. Highly selective aldose reductase inhibitors. 1. 3-(Arylalkyl)-2,4,5-trioxoimidazolidine-1-acetic acids. J Med Chem. 1996;39(9):1924–1927.
33. Tilekar K, Upadhyay N, Hess JD, Macias LH, Mrowka P, Aguilera RJ, Meyer-Almes F-J, Iancu CV, Choe J-y, Ramaa C. Structure guided design and synthesis of furyl thiazolidinedione derivatives as inhibitors of GLUT 1 and GLUT 4, and evaluation of their anti-leukemic potential. Eur J Med Chem. 2020;202:112603.
34. Bruno G, Costantino L, Curinga C, Maccari R, Monforte F, Nicolo F, Ottana R, Vigorita M. Synthesis and aldose reductase inhibitory activity of 5-arylidene-2,4-thiazolidinediones. Bioorg Med Chem. 2002;10(4):1077–1084.
35. Kaminskyy D, Kryshchyshyn A, Lesyk R. 5-Ene-4-thiazolidinones – an efficient tool in medicinal chemistry. Eur J Med Chem. 2017;140:542–594.
36. Xia Z, Knaak C, Ma J, Beharry ZM, McInnes C, Wang W, Kraft AS, Smith CD. Synthesis and evaluation of novel inhibitors of Pim-1 and Pim-2 protein kinases. J Med Chem. 2009; 52(1):74–86.
37. Stana A, Tiperciuc B, Duma M, Vlase L, Crişan O, Pîrnău A, Oniga O. Synthesis and antimicrobial activity of some new N-substituted-5-arylidene-thiazolidine-2,4-diones. J Heterocycl Chem. 2014;51(2):411–417.
38. Hurren KM, Dunham MW. Are thiazolidinediones a preferred drug treatment for type 2 diabetes? Expert Opin Pharmacother. 2021;22(2):131–133.
39. Othman DIA, Hamdi A, Tawfik SS, Elgazar AA, Mostafa AS. Identification of new benzimidazole-triazole hybrids as anticancer agents: multi-target recognition, in vitro and in silico studies. J Enzyme Inhib Med Chem. 2023;38(1):2166037.

40. Al-Sanea MM, Hamdi A, Mohamed AAB, El-Shafey HW, Moustafa M, Elgazar AA, Eldehna WM, Ur Rahman H, Parambi DGT, Elbargisy RM, et al. New benzothiazole hybrids as potential VEGFR-2 inhibitors: design, synthesis, anticancer evaluation, and in silico study. J Enzyme Inhib Med Chem. 2023;38:2166036.
41. El-Senduny FF, Elgazar A, Alwasify HA, Abed A, Foda M, Abouzeid S, Lewerenz L, Selmar D, Badria F. Bio-evaluation of untapped alkaloids from *Vinca minor* enriched by methyl jasmonate induced stress: an integrated approach. Planta Med. 2023.
42. Hamdi A, El-Shafey HW, Othman DIA, El-Azab AS, AlSaif NA, Abdel-Aziz AAM. Design, synthesis, antitumor, and VEGFR-2 inhibition activities of novel 4-anilino-2-vinyl-quinazolines: molecular modeling studies. Bioorg Chem. 2022;122:105710.
43. Hamdi A, Elhusseiny WM, Othman DI, Haikal A, Bakheit AH, El-Azab AS, Al-Agamy MH, Alaa A-M. Synthesis, antitumor, and apoptosis-inducing activities of novel 5-arylidenethiazolidine-2,4-dione derivatives: histone deacetylases inhibitory activity and molecular docking study. Eur J Med Chem. 2022;244:114827.
44. Othman DI, Hamdi A, Abdel-Aziz MM, Elfeky SM. Novel 2-arylthiazolidin-4-one-thiazole hybrids with potent activity against *Mycobacterium tuberculosis*. Bioorg Chem. 2022;124:105809.
45. Islam MS, Al-Majid AM, Azam M, Verma VP, Barakat A, Haukka M, Elgazar AA, Mira A, Badria FA. Construction of spirooxindole analogues engrafted with indole and pyrazole scaffolds as acetylcholinesterase inhibitors. ACS Omega. 2021;6(47):31539–31556.
46. Al-Sanea MM, Hamdi A, Brogi S, Tawfik SS, Othman DIA, Elshal M, Ur Rahman H, Parambi DGT, Elbargisy RM, Selim S, et al. Design, synthesis, and biological investigation of oxadiazolyl, thiadiazolyl, and pyrimidinyl linked antipyrine derivatives as potential non-acidic anti-inflammatory agents. J Enzyme Inhib Med Chem. 2023;38(1):2162511.
47. Al-Sanea MM, Chilingaryan G, Abelyan N, Mamikonyan M, Gasparyan H, Hovhannisyan S, Hamdi A, Ali AR, Selim S, Mohamed AA. Combination of ligand and structure based virtual screening approaches for the discovery of potential PARP1 inhibitors. PLOS One. 2022;17(9):e0272065.
48. Martinez A, Alonso M, Castro A, Dorronsoro I, Gelpí JL, Luque FJ, Pérez C, Moreno FJ. SAR and 3D-QSAR studies on thiadiazolidinone derivatives: exploration of structural requirements for glycogen synthase kinase 3 inhibitors. J Med Chem. 2005;48(23):7103–7112.
49. Kumar H, Aggarwal N, Marwaha MG, Deep A, Chopra H, Matin MM, Roy A, Emran TB, Mohanta YK, Ahmed R, et al. Thiazolidin-2,4-dione scaffold: an insight into recent advances as antimicrobial, antioxidant, and hypoglycemic agents. Molecules. 2022;27(19):6763.
50. Long N, Le Gresley A, Wren SP. Thiazolidinediones: an in-depth study of their synthesis and application to medicinal chemistry in the treatment of diabetes mellitus. ChemMedChem. 2021;16(11):1717–1736.
51. Kousaxidis A, Petrou A, Lavrentaki V, Fesatidou M, Nicolaou I, Geronikaki A. Aldose reductase and protein tyrosine phosphatase 1B inhibitors as a promising therapeutic approach for diabetes mellitus. Eur J Med Chem. 2020;207:112742.
52. Lee YS, Chen Z, Kador PF. Molecular modeling studies of the binding modes of aldose reductase inhibitors at the active site of human aldose reductase. Bioorg Med Chem. 1998;6(10):1811–1819.
53. Wilson DK, Tarle I, Petrash JM, Quiocho FA. Refined 1.8 A structure of human aldose reductase complexed with the potent inhibitor Zopolrestat. Proc Natl Acad Sci USA. 1993;90(21):9847–9851.
54. Aungst BJ. Optimizing oral bioavailability in drug discovery: an overview of design and testing strategies and formulation options. J Pharm Sci. 2017;106(4):921–929.
55. Lipinski CA, Lombardo F, Dominy BW, Feeney PJ. Experimental and computational approaches to estimate solubility and permeability in drug discovery and development settings. Adv Drug Deliv Rev. 1997;23(1–3):3–25.
56. Veber DF, Johnson SR, Cheng H-Y, Smith BR, Ward KW, Kopple KD. Molecular properties that influence the oral bioavailability of drug candidates. J Med Chem. 2002;45(12):2615–2623.
57. El-Shafey HW, Gomaa RM, El-Messery SM, Goda FE. Quinazoline based HSP90 inhibitors: synthesis, modeling study and ADME calculations towards breast cancer targeting. Bioorg Med Chem Lett. 2020;30(15):127281.
58. Wang R, Fu Y, Lai L. A new atom-additive method for calculating partition coefficients. J Chem Inf Comput Sci. 1997;37(3):615–621.
59. Peprah K, Zhu XY, Eyunni SVK, Etukala JR, Setola V, Roth BL, Ablordeppey SY. Structure–activity relationship studies of SYA 013, a homopiperazine analog of haloperidol. Bioorg Med Chem. 2012;20(5):1671–1678.
60. Wang X, Shen Y, Wang S, Li S, Zhang W, Liu X, Lai L, Pei J, Li H. PharmMapper 2017 update: a web server for potential drug target identification with a comprehensive target pharmacophore database. Nucleic Acids Res. 2017;45(W1):W356–W360.
61. Nnyigide OS, Nnyigide TO, Lee S-G, Hyun K. Modeling, protein repair and analysis server: a web server to repair PDB structures, add missing heavy atoms and hydrogen atoms, and assign secondary structures by amide interactions. J Chem Inf Model. 2022;62(17):4232–4246.
62. Laskowski RA, Swindells MB. LigPlot+: multiple ligand–protein interaction diagrams for drug discovery. J Chem Inf Model. 2011;51(10):2778–2786.
63. Dallakyan S, Olson AJ. Small-molecule library screening by docking with PyRx. Methods Mol Biol. 2015;1263:243–250.
64. Elimam DM, Elgazar AA, El-Senduny FF, El-Domany RA, Badria FA, Eldehna WM. Natural inspired piperine-based ureas and amides as novel antitumor agents towards breast cancer. J Enzyme Inhib Med Chem. 2022;37(1):39–50.